Inorg. Chem. **2008**, *47*, 6184−6194

Coordination Polymers from the Self-Assembly of Silver(I) Salts and Two Nonlinear Aliphatic Dinitrile Ligands, *cis*-1,3-Cyclopentanedicarbonitrile and *cis*-1,3-Bis(cyanomethyl)cyclopentane: Synthesis, Structures, and Photoluminescent Properties

Emerson D. Genuis,[†] Joel A. Kelly,[‡] Malay Patel, Robert McDonald,[§] Michael J. Ferguson,[§] and Grace Greidanus-Strom*

Department of Chemistry, The King's University College, 9125 50 St. Edmonton, Alberta, Canada T6B 2H3

Received January 18, 2008

Six coordination polymers with aliphatic dinitrile ligands, $\{[Ag(cpdcn)_2]ClO_4\}_n$ (**6a**), $\{[Ag(cpdcn)_2]PF_6\}_n$ (**6b**), $\{[Ag(cpdcn)_2]SbF_6\}_n$ (**6c**, cpdcn = *cis*-1,3-cyclopentanedicarbonitrile), $\{[Ag(bcmcp)_2]\ ClO_4\}_n$ (**7a**), $\{[Ag(bcmcp)_2]PF_6\}_n$ (**7b**), $\{[Ag(bcmcp)_2]SbF_6\}_n$, (**7c**, bcmcp = *cis*-1,3-bis(cyanomethyl)cyclopentane) have been synthesized and structurally characterized by IR spectroscopy, differential scanning calorimetry (DSC), thermogravimetric analysis (TGA) and X-ray crystallography. Both ligands used in this study are *meso*-compounds; while the ligand cpdcn is structurally rigid, the ligand bcmcp has greater conformational flexibility. X-ray crystallography has revealed that structures **6a-c** consist of chiral 1D-polymers. The structure of complexes **7a** and **7b** are best described as a 2D chiral (4,4) square mesh with 3-fold parallel interpenetration. Surprisingly, complex **7c** was characterized to be an achiral 1D coordination polymer. The synthesis of the ligands, IR spectra of the free and coordinated CN groups, DSC and TGA, and the photoluminescent properties of complexes **6a**−**c** and **7a**−**c** are also discussed.

Introduction

In the field of supramolecular chemistry, the construction of coordination polymers or metal-organic frameworks is a fascinating, beautiful, and rapidly growing area of interest.[1] Chemists have witnessed the self-assembly of elaborately designed building blocks which incorporate metal ions bridged with organic spacers.[2,3] A wide variety of infinite networks (1D, 2D, or 3D) with a high degree of order have been reported possessing a wide range of topologies and in many cases exhibiting interesting properties and potential uses such as microporosity, host−guest chemistry, molecular magnetism, nonlinear optical behavior, ion exchange, and catalysis, resulting in the development of optical, magnetic and electronic devices and more.[2,4]

In much of the literature describing Ag(I) coordination polymers to nitrogen-based ligands, rigid ligands with fixed bridging angles, such as bipyridine, pyrimidine, pyrazine, and pyridazine have been employed, as these ligands lend themselves toward a more straightforward design of network structures.[5,6] It has been known since 1959 that linear aliphatic dinitriles coordinate with metal salts to give coordination networks.[7] In contrast to rigid ligands, ditopic ligands with conformationally flexible aliphatic linkages offer

* To whom correspondence should be addressed. E-mail: grace.strom@kingsu.ca. Phone: 780-465-3500 ext. 8073.
† Current address: Faculty of Medicine and Dentistry, University of Alberta, Edmonton, Alberta, Canada T6G 2R7.
‡ Current address: Department of Chemistry, University of Alberta, Edmonton, Alberta, Canada T6G 2G2.
§ Current address: X-ray Crystallography Laboratory, Department of Chemistry, University of Alberta, Edmonton, Alberta, Canada T6G 2G2.

(1) Braga, D.; Grepioni, F.; Orpen, A. G. *Crystal Engineering: From Molecules and Crystals to Materials*; Kluwer Academic Publishers: Dordtrecht, The Netherlands, 1999.
(2) Abd-El-Aziz, A. S.; Manners, I. *Frontiers in transition metal-containing polymers*; John Wiley: Hoboken, NJ, 2007.
(3) Braga, D.; Grepioni, F. *Making Crystals by Design: Methods, Techniques and Applications.*; Wiley-VCH: New York, 2007; p 362.
(4) Mueller, U.; Schubert, M.; Teich, F.; Puetter, H.; Schierle-Arndt, K.; Pastre, J. *J. Mat. Chem.* **2006**, *16*, 626.
(5) Khlobystov, A. N.; Blake, A. J.; Champness, N. R.; Lemenovskii, D. A.; Majouga, A. G.; Zyk, N. V.; Schroder, M. *Coord. Chem. Rev.* **2001**, *222*, 155.
(6) Chen, C. L.; Kang, B. S.; Su, C. Y. *Aust. J. Chem.* **2006**, *59*, 3.

10.1021/ic800069f CCC: $40.75
Published on Web 06/24/2008

significant orientational diversity to the coordination polymer. This, in addition to the many factors that affect topology (e.g., counterions, solvents, oxidation state of metal, metal to ligand ratio),[8] makes prediction of resultant complexes challenging. In the past decade, reactions of various straight chain aliphatic dinitrile ligands with silver salts have been investigated, as Ag(I) easily adapts to various coordination geometries (the most common are linear, trigonal planar, and tetrahedral). Significantly, a possible trend was reported by G. Ciani resulting from a systematic study on the reactions of short to long-chain dinitriles with silver salts. When using a 1:2 metal to ligand ratio, they witnessed two distinct topologies (2D square layers and interpenetrating 3D diamondoids) that appeared to be directly affected by the number of methylene linkers in the tether between the two nitrile groups.[9–11] Interpenetrating 3D diamondoid networks of 6^6 topology occurred when an even number of carbon atoms were present in the ligand backbone, as evidenced by structures of $[Ag(dinitrile)_2]^+$ complexes with ligands 1,4-dibutanedinitrile, 1,6-hexanedinitrile (adiponitrile),[11] 1,10-decanedinitrile (sebacodinitrile)[9] and 1,12-dodecanedinitrile.[10] The noted exceptions were $[Ag(adiponitrile)_2]ClO_4$, which has a 2D square structure and $[Ag(sebacodinitrile)_2]^+$ complexes which demonstrates 3D diamondoid, 3D $SrAl_2$-type and 2D layers.[10] The choice of counterion appeared to affect the degree of interpenetration more (from 4-fold to 12-fold) than to influence the network topology.[9] Other dinitrile ligands, mostly with an odd number of carbons in the backbone, such as 1,5-pentanedinitrile, 1,7-heptanedinitrile, 1,8-octanedinitrile, and 1,9-nonanedinitrile favor 2D layer structures.[11] An additional anomaly to this trend was reported in a study undertaken by Hardie et al., who reported that in the case of $[Ag((\mu\text{-}1,3\text{-propanedinitrile})_2]BF_4$, a chiral 2-fold interpenetrating 3D diamondoid structure is observed.[12]

Ciani et al. also examined the effect of $CF_3SO_3^-$ as a weakly coordinating counterion on the resultant polymer topology when less than two equivalents of ligand are used. In all cases the counterion was observed to weakly interact with the Ag metal centers.[9] This study is complemented by the work of Hardie et al., who illustrate that even large, weakly coordinating counterions, such as carborane anions, also result in weak interactions with silver yielding structures with either discrete, chain or 3D lattice structures.[12]

Additional studies have appeared where aliphatic dinitrile ligands containing ether,[13] thioether,[14] or amine[15,16] groups in the ligand backbone have been coordinated to Ag(I) to yield coordination polymers. Of note, the authors observed that counterions play a significant role in the resulting polymer topology. For example, despite using two noncoordinating anions of relatively similar size (ClO_4^- and BF_4^-), greatly differing 3D topology was observed for the complexes $[Ag(oxidipropionitrile)_2]^+$.[13]

Absent from this body of work is a direct comparison of a structurally rigid aliphatic dinitrile ligand to one with an increase in conformational flexibility. It is our intent to devise new ligands that compare structurally rigid aliphatic tethers between two nitrile groups to analogous ligands with incremental increases in degrees of freedom. In so doing we hope to determine the correct balance between conformational flexibility, ligand rigidity, and tether length to be able to produce monomeric Ag(I) complexes[17] in addition to gaining predictive insight into polymer topology. Herein we report the first set of ligands in this investigation, the coordination of two nonlinear aliphatic dinitrile ligands with *meso*-stereochemistry (shown below), *cis*-1,3-cyclopentanedicarbonitrile (cpdcn), **1** and *cis*-1,3-bis(cyanomethyl)cyclopentane (bcmcp), **2** to the silver salts, $AgClO_4$, $AgPF_6$, and $AgSbF_6$. The self-assembly of $AgClO_4$, $AgPF_6$, and $AgSbF_6$ with structurally rigid cpdcn **1** yields in each case a chiral 1D coordination polymer that contains a tetrahedrally coordinated silver ion. The coordination of bcmcp **2** to Ag(I) ions also results in the formation of polymeric structures with tetrahedrally coordinated silver ions; however, counterions ClO_4^- and PF_6^- yield a chiral 2D (4,4) square mesh, whereas the SbF_6^- counterion surprisingly yields a nonchiral 1D coordination polymer.

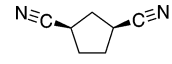

1 (cpdcn)

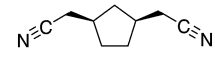

2 (bcmcp)

Experimental Section

Materials and Procedures. All starting materials were obtained from commercial sources and were of reagent grade. All manipulations on air sensitive compounds were performed under a nitrogen atmosphere using standard Schlenk techniques or in a nitrogen-filled drybox. IR spectra were recorded in the 400−4000 cm^{-1} region on a Nicolet Impact 400D spectrophotometer and are reported in reciprocal wave numbers (cm^{-1}) calibrated to the 1601 cm^{-1} absorption of polystyrene. Determinations were done on compounds applied as a thin film on KBr plates (referred to as "casts"), or as KBr pellets. Elemental analyses were performed by the University of Alberta Microanalysis Laboratories.

Differential scanning calorimetry (DSC) measurements were made on a Perkin-Elmer Pyris 1 DSC in the temperature range between 20 and 450 °C at a heating rate of 15 °C min^{-1} using standard aluminum sample pans. Thermogravimetric analyses (TGAs) were studied by a Perkin-Elmer Pyris 1 TGA in a N_2 atmosphere in the temperature range between 30 and 500 °C at a heating rate of 15 °C min^{-1} using Al_2O_3 crucibles.

Photoluminescence measurements were performed at room temperature in the solid state by casting a powdered sample onto a silicon wafer using acetone as the solvent. In the spectrometer setup, a 4w Nd:YAG laser (266 nm, 20 Hz, 20 ns, 3.3 mJ/pulse)

(7) Kinoshita, Y.; Matsubara, I.; Saito, Y. *Bull. Chem. Soc. Jpn.* **1959**, *32*, 1216.
(8) Patra, G. K.; Goldberg, I. *Cryst. Growth Des.* **2003**, *3*, 321.
(9) Carlucci, L.; Ciani, G.; Proserpio, D. M.; Rizzato, S. *Chem.—Eur. J.* **2002**, *8*, 1520.
(10) Carlucci, L.; Ciani, G.; Macchi, P.; Proserpio, D. M.; Rizzato, S. *Chem.—Eur. J.* **1999**, *5*, 237.
(11) Carlucci, L.; Ciani, G.; Proserpio, D. M.; Rizzato, S. *Crystengcomm* **2002**, 413.
(12) Westcott, A.; Whitford, N.; Hardie, M. J. *Inorg. Chem.* **2004**, *43*, 3663.
(13) Zhang, J.; Li, Z.-J.; Kang, Y.; Qin, Y.-Y.; Cheng, J.-K.; Yao, Y.-G. *Cryst. Growth Des.* **2005**, *5*, 73.
(14) Cheng, J. K.; Zhang, J.; Kang, Y.; Qin, Y. Y.; Li, Z. J.; Yao, Y. G. *Polyhedron* **2004**, *23*, 2209.
(15) Erxleben, A. *CrystEngComm* **2002**, 472.
(16) Kang, Y. J.; Lee, S. S.; Park, K. M.; Lee, S. H.; Kang, S. O.; Ko, J. J. *Inorg. Chem.* **2001**, *40*, 7027.
(17) Angelici, R. J.; Quick, M. H.; Kraus, G. A.; Plummer, D. T. *Inorg. Chem.* **1982**, *21*, 2178.

was used to excite luminescence of the sample, and two high reflectivity mirrors (HR 268 nm) were placed in front of the laser to direct the laser beam. Collimating spherical mirrors were used to collect luminescent light emitted from the sample. A filter set was placed in front of the 400 μm diameter optical fiber to remove the scattered laser light. A spectrometer (Ocean optics, bandwidth 200−850 nm, 8 nm resolution, 200 μm entrance slit, coupled to the optical fiber) was placed after the filter set to collect the photoluminescence spectrum.

X-ray Structure Determination. X-ray crystallography intensity data were collected on a Bruker PLATFORM/SMART 1000 CCD at −80 °C with graphite-monochromated Mo Kα radiation (λ = 0.71073 Å). Data were corrected for Lorenztian and polarization effects; absorption corrections were applied to the data using multiscan methods. All crystal structures were solved using direct methods (SHELXS-86) and refined against F^2 using SHELXL-93. All non-hydrogen atoms were refined anisotropically.

The crystal used for data collection of **6a** was found to display nonmerohedral twinning. Both components of the twin were indexed with the program CELL_NOW (Bruker AXS Inc., Madison, WI, 2004). The first twin component can be related to the second component by 180° rotation about the [0 0 1] axis in both real and reciprocal space. Integrated intensities for the reflections from the two components were written into a SHELXL-93 HKLF 5 reflection file with the data integration program SAINT (version 7.06A), using all reflection data (exactly overlapped, partially overlapped, and nonoverlapped).

In complex **6c**, the SbF_6 anions are disordered and distances involving the minor occupancy (30%) were constrained to be equal (within 0.001 Å). In complex **7a**, the ClO_4 anions are disordered and were constrained to be equal (within 0.001 Å). In complexes **7a**-**c**, the ligand is disordered and the geometry of the minor component of the disordered ligand was restrained to be the same as that of the major component (70%) by the use of the SHELXL SAME instruction during refinement. The N2−C9A and N2−C9B distances were restrained to be equal. In **7b**, the geometry of the PF_6 anion was restrained to be octahedral and in **7c**, the SbF_6 anion was found to be rotationally disordered about the 4-fold rotational axis. This could be modeled by splitting the equatorial fluorine atom position into three distinct sites, (F3A, F3B, and F3C) with occupancies of 50%, 30%, and 20%, respectively. The Sb−F distances were restrained to be equal, and the angles between adjacent sites were restrained to be 30°.

Caution! *Although no problems were encountered in this study, transition-metal perchlorate complexes are potentially explosive and should be handled with proper precautions.*

Preparations. *cis*-1,3-Cyclopentanedicarbaldehyde, 3. The preparation of dialdehyde **3** was modified from a literature procedure as follows:[18] a 500 mL round-bottomed flask containing a rapidly stirring magnetic bar and 100 mL of dichloromethane were charged with $KMnO_4$ (53.0 g, 335.4 mmol) and $CuSO_4 \cdot 5H_2O$ (53.0 g, 212.3 mmol); 5 mL of distilled water was added to this suspension. Norbornene (10.0 g, 121.7 mmol) was dissolved in dichloromethane (50 mL) and slowly added to the oxidant mixture followed by 25 mL of *t*-butanol. After 3 h the reaction mixture was filtered through Celite and washed with 50 mL of saturated brine. The brine was then backwashed with dichloromethane (2 × 25 mL). The combined organic layers were dried over $MgSO_4$, and the solvent was removed by rotary evaporation under ambient conditions to yield 8.90 g (58%) of a colorless oil. Dialdehyde **3** is unstable at room temperature and was used in further synthetic procedures immediately following rotary evaporation.

***cis*-1,3-Cyclopentanedicarbonitrile, 1.** A clean, dry 250 mL round-bottomed flask are charged with freshly prepared *cis*-1,3-cyclopentanedicarbaldehyde **3** (3.2 g, 25.3 mmol), THF (16 mL), and concentrated ammonium hydroxide (150 mL). The mixture was placed in a 20 °C water bath and 16.0 g (63.0 mmol) of iodine was added in small aliquots over 20 min. After 2 h the reaction was quenched by addition of 10% $Na_2S_2O_3$ (30 mL) and stirred for 15 min. The reaction mixture was rotary evaporated to remove THF from the reaction mixture and the product was then extracted into dichloromethane (5 × 30 mL). The combined organic layers were dried over $MgSO_4$, filtered through Celite and evaporated to dryness. Pure product was obtained by passing the crude product through a silica gel bed (∼2 cm) and eluted with dichloromethane. The solvent was removed by rotary evaporation to obtain as a clear colorless oil, *cis*-1,3-cyclopentanedicarbonitrile **2** (2.42 g, 79.6%). ^{1}H NMR (400.1 MHz, C_3D_6O) δ 3.09 (m, 2H), 2.59 (dt, J = 8.0, 8.2 Hz, 2H), 2.19 (m, 2H), 2.048 (m, 2H). ^{13}C NMR (100 MHz, C_3D_6O) δ 122.5, 36.1, 31.2, 27.3. IR (cm^{-1}, cast): 2984(m), 2241(m), 1734(s), 1451(m), 1245(s), 1046(m). Anal. Calcd for $C_7H_8N_2$: C, 70.00; H, 6.70; N, 23.30; found C, 70.16; H, 6.88; N, 23.09.

***cis*-1,3-Bis(hydroxymethyl)cyclopentane, 4.** To a clean, dry 500 mL round-bottomed flask under a nitrogen atmosphere was added freshly prepared *cis*-1,3-cyclopentanedicarbaldehyde **3** (4.17 g, 33.1 mmol) and 150 mL of deoxygenated methanol. The reaction mixture was cooled to 0 °C and $NaBH_4$ (4.93 g, 130.3 mmol) was added in small aliquots to avoid the reaction temperature from rising above 10 °C. The reaction mixture was left to warm to room temperature and stirred an additional 14 h under a nitrogen atmosphere. Distilled water (25 mL) was added to the reaction mixture to quench any remaining $NaBH_4$ and then rotary evaporated to remove methanol from the solution. The remaining mixture was extracted with dichloromethane (5 × 25 mL); the organic fractions were combined and dried over $MgSO_4$. The solvent was removed under reduced pressure to yield pure *cis*-1,3-bis(hydroxymethyl)cyclopentane **4** (3.24 g, 75%) as a colorless oil. ^{1}H NMR (400.1 MHz, $CDCl_3$) δ 3.51 (m, 4H), 2.68 (s, 2H), 2.14 (m, 2H), 1.95 (dt, J = 12.6, 7.8 Hz, 1H), 1.73 (m, 2H), 1.34 (m, 2H), 0.93 (dt, J = 12.6, 9.1 Hz, 1H). ^{13}C NMR (100 MHz, $CDCl_3$) δ 67.0, 42.3, 32.9, 28.3. Anal. Calcd for $C_7H_{14}O$: C, 64.58; H, 10.84; found C, 64.45; H, 10.75.

***cis*-1,3-Bis(4-toluenesulfonyloxymethyl)cyclopentane, 5.** To a cooled (<20 °C) solution of pyridine (125 mL) and diol **4** (3.24 g, 24.9 mmol) was added *p*-toluenesulfonyl chloride (14.24 g, 74.8 mmol). The reaction was placed under an inert atmosphere and allowed to stir overnight at room temperature. The pyridine was removed by rotary evaporation leaving a white solid residue in the flask. The products were partitioned between 2 M HCl and dichloromethane, the organic layer was removed, and the aqueous layer was washed with dichloromethane (4 × 30 mL). Saturated $NaHCO_3$ (25 mL) was added to the combined organic layers to quench any residual *p*-toluenesulfonyl chloride. The dichloromethane layer was removed, and the aqueous layer was re-extracted with dichloromethane (4 × 25 mL). The organic fractions were combined and dried over $MgSO_4$. The solvent was removed by rotary evaporation leaving a white powder. The product was further purified by washing with diethyl ether and dried to yield *cis*- 1,3-bis(4-toluenesulfonyloxymethyl)cyclopentane **5** (7.20 g, 66%). ^{1}H NMR (400.1 MHz, $CDCl_3$) δ 7.78 (d, J = 8.8 Hz, 4H), 7.36 (d, J = 8.1 Hz, 4H), 3.88 (m, 4H), 2.47 (s, 6H), 2.24 (m, 2H), 1.91 (dt, J = 12.9, 7.33 Hz, 1H), 1.72 (m, 2H), 1.28 (m, 2H), 0.84 (dt, J = 12.9, 9.6 Hz, 1H). ^{13}C NMR (100 MHz, $CDCl_3$) δ 144.9,

(18) Goksu, S.; Altundas, R.; Sutbeyaz, Y. *Synth. Commun.* **2000**, *30*, 1615.

132.9, 129.9, 127.9, 73.5, 38.7, 32.5, 27.9, 21.7. IR (cm^{-1}, cast): 3095(w), 2950(m), 1920(w), 1595(m), 1360(s), 1180(s), 950(s), 805(s). Anal. Calcd for $C_{21}H_{26}S_2O_6$: C, 57.51; H, 5.98; S, 14.6; found C, 57.34; H, 5.92; S, 14.54.

***cis*-1,3-Bis(cyanomethyl)cyclopentane, (bcmcp), 2.** To a 3:1 DMF/H_2O solution (75 mL) was added 7.20 g (37.8 mmol) of ditosyl **5**. The solution was heated to 150 °C and an excess of KCN (13 g) was added to the reaction mixture. After 14 h, the reaction mixture was cooled to room temperature, and an additional 10 mL of H_2O was added to the solution. The reaction mixture was extracted with diethyl ether (6 × 25 mL), and the combined organic fractions were dried over $MgSO_4$. The organic solvents were removed by rotary evaporation. The resulting pale yellow liquid was further purified by flash chromatography, ramping from hexane to pure dichloromethane as the eluent, to yield compound **2** in 85% yield (2.07 g). ^{1}H NMR (400 MHz, C_3D_6O) δ 2.54 (d, J = 8.00 Hz, 4H), 2.30 (m, 2H), 2.14 (dt, J = 6.6, 11.6 Hz, 1H), 1.92 (m, 2H), 1.47 (m, 2H), 1.11 (dt, J = 10.6, 11.0 Hz, 1H). ^{13}C NMR (100 MHz, C_3D_6O) δ 119.8, 39.0, 36.98, 31.21, 22.49. IR (cm^{-1}, cast): 2953(s), 2869(m), 2245(m), 1424(m), 1364(w). Anal. Calcd for $C_9H_{12}N_2$: C, 72.94; H, 8.16; N, 18.90; found C, 72.45; H, 8.29; N, 18.42.

Preparation of Silver(I) Complexes 6a−c. All complexes were prepared by a similar procedure. *cis*-1,3-Cyclopentanedicarbonitrile **1** was dissolved in ethanol (2.1 equiv, ∼0.2 M) and layered over an ethanolic solution containing AgX (1 equiv, ∼0.15 M, X = ClO_4^- **6a**, PF_6^- **6b**, SbF_6^- **6c**). The solutions were left to diffuse into each other and evaporate. The resulting solid was washed with THF to remove excess ligand and any trace impurities, taken up in acetone, and filtered through a short column of Celite. Removal of the solvent yielded a pure complex. Deviations from this procedure are noted for each individual complex.

{[Ag(cpdcn)$_2$]ClO_4}$_n$, 6a. Yield: 96%. Crystallographic material was obtained by dissolving the product in a minimum amount of acetone and allowing the solvent to slowly evaporate. ^{1}H NMR (400.1 MHz, C_3D_6O): δ 2.04−2.19 (m, 3H), 2.24 (m, 2H), 2.65 (dt, J = 8.1, 13.1 Hz, 1H), 3.16 (m, 2H). ^{13}C NMR (100 MHz, C_3D_6O): 27.16, 30.06, 35.18, 121.88. IR (cm^{-1}, KBr pellet): 2257. Anal. Calcd for $C_{14}H_{16}N_4AgClO_4$: C, 37.57; H, 3.60; N, 12.52. Found C, 37.70; H, 3.74; N, 12.54. Melting point: 190 °C.

{[Ag(cpdcn)$_2$]PF_6}$_n$, 6b. Yield: 93%. Crystallographic material was obtained by dissolving the product in a minimum amount of 2-butanone and allowing the solvent to slowly evaporate. ^{1}H NMR (400.1 MHz, C_3D_6O): δ 2.02−2.16 (m, 3H), 2.23 (m, 2H), 2.64 (dt, J = 8.1, 13.1 Hz, 1H), 3.15 (m, 2H). ^{13}C NMR (100 MHz, C_3D_6O): δ 27.15, 30.05, 35.16, 121.90. IR (cm^{-1}, KBr pellet): 2241. Anal. Calcd for $C_{14}H_{16}N_4AgPF_6$: C, 34.10; H, 3.27; N, 11.36. Found C, 33.88; H, 3.40; N, 11.43. Melting point: 176 °C.

{[Ag(cpdcn)$_2$]SbF_6}$_n$, 6c. Yield: 99%. This procedure was performed under an inert atmosphere; the product is air-stable. Crystallographic material was obtained by dissolving the product in a minimum amount of acetone and layering this solution with an equivalent amount of 2-butanone and allowing the solvent to slowly evaporate. ^{1}H NMR (400.1 MHz, C_3D_6O): δ 2.04−2.17 (m, 3H), 2.24 (m, 2H), 2.65 (dt, J = 8.1, 13.1 Hz, 1H), 3.16 (m, 2H). ^{13}C NMR (100 MHz, C_3D_6O): δ 27.17, 30.06, 35.16, 121.96. IR (cm^{-1}, KBr pellet): 2241. Anal. Calcd for $C_{14}H_{16}N_4AgSbF_6$: C, 28.80; H, 2.76; N, 9.60. Found C, 29.28; H, 2.95; N, 9.98. Melting point: 238 °C.

Preparation of Silver(I) Complexes 7a−c. All complexes were prepared by a similar procedure. *cis*-1,3-Bis(cyanomethyl)cyclopentane **2** was dissolved in ethanol (2.1 equiv, ∼0.2 M) and layered over an ethanolic solution containing AgX (1 equiv, ∼0.15 M, X = ClO_4^- 7a, PF_6^- 7b, SbF_6^- 7c). The solutions were left to diffuse into each other and evaporate. As the solvent began to evaporate, crystalline material formed at the bottom of the flask. After approximately two-thirds of the solvent had evaporated, the remaining solvent was decanted, and the residue dried. Deviations from this procedure are noted for each individual complex.

{[Ag(bcmcp)$_2$]ClO_4}$_n$, 7a. The procedure yielded crystallographic material in 88% yield. ^{1}H NMR (400.1 MHz, C_3D_6O): δ 1.14 (dt, J = 10.1, 12.4 Hz, 1H), 1.51 (m, 2H), 1.95 (m, 2H), 2.19 (dt, J = 7.1, 12.1 Hz, 1H), 2.34 (m, 2H), 2.61 (d, J = 6.6 Hz, 4H). ^{13}C NMR (100 MHz, C_3D_6O): δ 21.74, 30.46, 36.10, 38.19, 119.51. IR (cm^{-1}, KBr pellet): 2269. Anal. Calcd for $C_{18}H_{24}N_4AgClO_4$: C, 42.92; H, 4.80; N, 11.12. Found C, 42.79; H, 4.84; N, 10.85. Melting point: 89 °C.

{[Ag(bcmcp)$_2$]PF_6}$_n$, 7b. Yield: 94%. Crystallographic material was obtained by dissolving the product in a minimum amount of acetone, layering the solution with an equivalent amount of ethanol, and allowing the solvent to slowly evaporate. ^{1}H NMR (400.1 MHz, C_3D_6O): δ 1.13 (dt, J = 10.1, 12.1 Hz, 1H), 1.51 (m, 2H), 1.95 (m, 2H), 2.19 (dt, J = 6.8, 12.2 Hz, 1H), 2.33 (m, 2H), 2.58 (d, J = 6.8 Hz, 4H). ^{13}C NMR (100 MHz, C_3D_6O): δ 21.73, 30.46, 36.07, 38.16, 119.54. IR (cm^{-1}, KBr pellet): 2247. Anal. Calcd for $C_{18}H_{24}N_4AgPF_6$: C, 39.36; H, 4.40; N, 10.20. Found C, 39.78; H, 4.68; N, 10.34. Melting point: 135 °C.

{[Ag(bcmcp)$_2$]SbF_6}$_n$, 7c. This procedure was performed under an inert atmosphere; the product is air-stable. The solid was removed from the inert atmosphere, washed with ethanol, taken up in acetone, and filtered through a short column of Celite. The solvent was removed yielding complex **7c** in 97% yield. Crystallographic material was obtained by dissolving the product in a minimum amount of acetone, layering the solution with an equivalent amount of ethanol, and allowing the solvent to slowly evaporate. ^{1}H NMR (400.1 MHz, C_3D_6O): δ 1.14 (dt, J = 10.1, 12.4 Hz, 1H), 1.51 (m, 2H), 1.95 (m, 2H), 2.19 (dt, J = 7.1, 12.1 Hz, 1H), 2.34 (m, 2H), 2.60 (d, J = 6.8 Hz, 4H). ^{13}C NMR (100 MHz, C_3D_6O): δ 21.74, 30.47, 36.12, 38.20, 119.42. IR (cm^{-1}, KBr pellet): 2248. Anal. Calcd for $C_{18}H_{24}N_4AgSbF_6$: C, 33.80; H, 3.78; N, 8.75. Found C, 34.29; H, 4.04; N, 8.38. Melting point: 117 °C.

Results and Discussion

Synthesis of the Ligands. The two dinitrile ligands used in this work, *cis*-1,3-cyclopentanedicarbonitrile (cpdcn) **1** and *cis*-1,3-bis(cyanomethyl)cyclopentane (bcmcp) **2**, both contain two asymmetric centers related to each other through an internal plane of symmetry rendering the ligand a *meso*-compound. The structural difference between the two ligands is the extra methylene group in the ligand backbone separating the nitrile from the five-membered ring. While both ligands are ditopic, the backbone between the two nitrile groups in cpdcn **1** is structurally quite rigid, and the coordination of this ligand to silver(I) is not expected to be influenced by many of the factors that affect polymer topology, such as steric effects.[8] Relative to cpdcn **1**, the additional methylene groups in bcmcp **2** affords greater flexibility, leading to greater diversity of the extended structure in the self-assembly of coordination complexes.

Ligand cpdcn **1** was synthesized in two steps from norbornene (Figure 1). Oxidative ring-opening of norbornene using $KMnO_4$ as the oxidant yielded dialdehyde **3**.[18] As dialdehyde **3** is unstable, it was immediately converted to

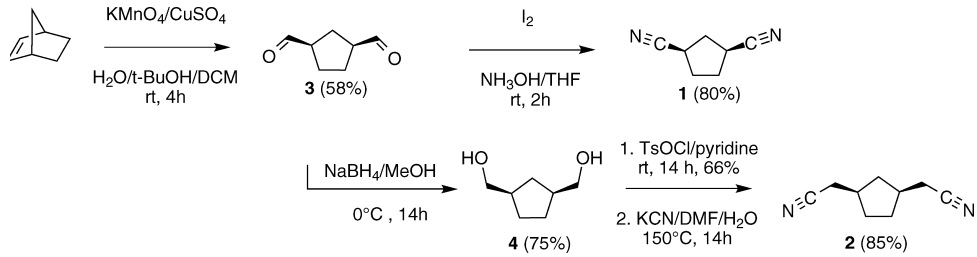

Figure 1. Synthesis of dinitrile ligands cpdcn **1** and bcmcp **2**.

Table 1. IR Data for Ligands cpdcn **1** and bcmcp **2** and Complexes **6a**−**c** and **7a**−**c**

		nitrile peak (cm^{-1})
cpdcn	**1**	2241
$\{[Ag(cpdcn)_2]ClO_4\}_n$	**6a**	2241
$\{[Ag(cpdcn)_2]PF_6\}_n$	**6b**	2242
$\{[Ag(cpdcn)_2]SbF_6\}_n$	**6c**	2241
bcmcp	**2**	2245
$\{[Ag(bcmcp)_2]ClO_4\}_n$	**7a**	2257
$\{[Ag(bcmcp)_2]PF_6\}_n$	**7b**	2247
$\{[Ag(bcmcp)_2]SbF_6\}_n$	**7c**	2248

cpdcn **1** using iodine as the oxidant in ammonia−water.[19] For the synthesis of bcmcp **2**, freshly prepared dialdehyde **3** is reduced using sodium borohydride, the resulting diol **4** is converted to ditosylate **5**, and under conditions for nucleophilic displacement, the tosylate group is converted to a nitrile to yield bcmcp **2**.

Synthesis of the Complexes. To prepare the complexes in this investigation $AgClO_4$, $AgPF_6$, and $AgSbF_6$ were dissolved in ethanol and mixed with ethanolic solutions of either cpdcn **1** or bcmcp **2** in a 1:2 ratio and allowed to evaporate, yielding a coordination polymer in each case as revealed by X-ray crystallography. All of the complexes generated in this study are very air-stable but are mildly light sensitive and should be stored in the dark.

General Characterization. IR Spectra. Nitrile absorption peaks in the IR spectra of complexes **6a**−**c** and **7a**−**c** and the ligands cpdcn **1** and bcmcp **2** are listed in Table 1. The presence of CN stretching frequencies around 2245 cm^{-1} indicate that all complexes contain nitrile groups. Consistent with previously reported ν_{CN} of polymeric complexes containing polydentate nitrile ligands,[12–14] the complexes formed using cpdcn ligand **1** indicate very little difference between the uncoordinated and coordinated ligand.[20] This suggests that the silver ions exert little influence on ν_{CN} values and that the shifts are consistent with "end-on" coordination geometry.[21] Unexpectedly, in comparing complexes formed using bcmcp ligand **2**, ν_{CN} is affected most through coordination to $AgClO_4$.

Melting Points, TGA and DSC. To assess the thermal stability of the polymers prepared in this study, TGA and DSC analyses as well as melting points were recorded. In all cases, TGA does not indicate stepwise removal of the coordinated ligands. In complexes **6a**−**c**, loss of ligand is observed shortly after the melting point has been reached and is not complete until temperatures reach above 300 °C. In complexes **7a**−**c**, the complex generally remains stable to approximately 50 °C beyond the melting point. Loss of all ligand occurs in one step, and ligand removal is not complete until temperatures near 350 °C. While DSC measurements were consistent with endothermic peaks measured near the melting points of the complexes, the numerous other endothermic and exothermic peaks observed in DSC thermograms recorded indicate that these complexes are subject to several solid-state transformations.

X-ray Single Crystals of Complexes 6a−**c.** Crystals of these three complexes were grown by slow evaporation of concentrated solutions. Despite using symmetric building blocks, complexes **6a**−**c** crystallize in monoclinic cells and are solved in chiral space groups. Whereas $\{[Ag(cpdcn)_2]ClO_4\}_n$ **6a** and $\{[Ag(cpdcn)_2]PF_6\}_n$ **6b** were solved in the chiral space group *P*2/*c*, $\{[Ag(cpdcn)_2]ClO_4\}_n$ **6c** is solved in the chiral space group *P*2/*n*. The crystallographic details are shown in Table 2. Supramolecular chirality is normally achieved following one of three strategies: (a) at least one component is asymmetric (e.g., the ligand); (b) a dissymmetrizing association of achiral components to create a chiral molecule; (c) the use of chiral environment to induce asymmetry into achiral components (e.g., chiral ionic liquids). Many chiral Ag(I) polymeric complexes have been reported recently using these three strategies.[22–24] Most chiral coordination polymers constructed from symmetric building blocks result from the self-assembly of asymmetric helical structures. To the best of our knowledge, this is the first example of the use of a *meso*-ligand to yield C_2-symmetric 1D coordination polymers (see Figure 2). In the polymeric structures of **6a**−**c**, the silver atoms form a remarkably linear straight line chain with only small deviations from linearity observed depending on the nature of the counterion (Y = ClO_4^- ∠ = 175.2°, Y = PF_6^- ∠= 176.1°, and Y = SbF_6^- ∠ =173.9°). In each case, the chain propagates along one of the crystallographic axes and the chains crystallize side by side to form sheets of 1D polymers. In the third dimension, the sheets are separated by rows of counterions (Figure 3). As evidenced by the high calculated density for the complexes (Y

(19) Talukdar, S.; Hsu, J.-L.; Chou, T.-C.; Fang, J.-M. *Tetrahedron Lett.* **2001**, *42*, 1103.

(20) IR frequency shifts of 30−70 cm^{-1} to higher frequencies are noted for monomeric complexes upon nitrile coordination. (a) Storhoff, B. N.; Lewis, H. C., Jr. *Coord. Chem. Rev.* **1977**, *23*, 1.

(21) Shimizu, K. D.; Rebek, J. *Proc. Natl. Acad. Sci. U.S.A.* **1996**, *93*, 4257.

(22) For a recent example using an asymmetric ligand ligand: (a) Ellsworth, J. M.; Su, C. Y.; Khaliq, Z.; Hipp, R. E.; Goforth, A. M.; Smith, M. D.; zur Loye, H. C. *J. Mol. Struct.* **2006**, *796*, 86.

(23) For a recent example of dissymmetrizing association: (a) Fu, Y. M.; Zhao, Y. H.; Lan, Y. Q.; Wang, Y.; Qiu, Y. Q.; Shao, K. Z.; Su, Z. M. *Inorg. Chem. Commun.* **2007**, *10*, 720.

(24) For a recent example of a chiral ionic liquid: (a) Lin, Z. J.; Slawin, A. M. Z.; Morris, R. E. *J. Am. Chem. Soc.* **2007**, *129*, 4880.

Table 2. Crystallographic Data for Complexes **6a**−**c** and **7a**−**c**

	formula					
	$\{[Ag(C_7H_8N_2)_2][ClO_4]\}_n$	$\{[Ag(C_7H_8N_2)_2][PF_6]\}_n$	$\{[Ag(C_7H_8N_2)_2][SbF_6]\}_n$	$\{[Ag(C_9H_{12}N_2)_2][ClO_4]\}_n$	$\{[Ag\{C_9H_{12}N_2)_2][PF_6]\}_n$	$\{[Ag(C_9H_{12}N_2)_2][SbF_6]\}_n$
formula weight	447.63	493.15	583.93	503.7	549.25	640.03
crystal dimensions (mm)	0.55 × 0.52 × 0.04	0.42 × 0.40 × 0.10	0.56 × 0.20 × 0.15	0.68 × 0.24 × 0.09	0.53 × 0.30 × 0.20	0.45 × 0.37 × 0.30
crystal system	monoclinic	monoclinic	monoclinic	orthorhombic	monoclinic	tetragonal
space group	*P*2/*c*	*P*2/*c*	*P*2/*n*	$C222_1$	*C*2	*I*4/*m*
a (Å)	11.3146 (8)	5.9443 (8)	12.7961 (16)	6.2270 (12)	15.889 (2)	11.2163 (10)
b (Å)	5.8353 (4)	11.3371 (15)	6.0721 (8)	15.598 (3)	6.2597 (8)	11.2163 (10)
c (Å)	12.9236 (9)	13.0729 (17)	13.6946 (18)	21.076 (4)	11.0006 (14)	18.286 (3)
β (deg)	95.3043 (14)	93.0094 (17)	119.5093 (15)		100.484 (2)	
V (Å^3)	849.61 (10)	879.8 (2)	926.0 (2)	2047.2 (7)	1075.8 (2)	2300.5 (5)
Z	2	2	2	4	2	4
T (K)	193	193	193	193	193	193
ρ_{calcd} (g•cm^{-3})	1.75	1.862	2.094	1.634	1.696	1.848
μ (mm^{-1})	1.369	1.302	2.578	1.147	1.074	2.085
2θ range	6.43°−52.74°	4.76°−52.74°	6.12°−52.68°	5.22°−49.32°	5.22°−52.76°	6.80°−52.50°
F(000)	448	488	560	1024	552	1248
independent reflections	13707	1813	1901	2099	2161	1204
observed reflections[a]	12275	1709	1783	1935	2152	1178
R_{int}	0	0.0236	0.013	0.0314	0.0236	0.0402
range of transmission factors	0.9473−0.5197	0.8808−0.6108	0.6984−0.3262	0.9038−0.5094	0.8138−0.5998	0.5352−0.4235
data[b]/restraints/parameters	13707/ 0/129	1813/ 0/120	1901/ 6[f]/132	2099/10[f,g]/172	2161/ 39[f]/233	1204/15[f]/115
$S^{b,c}$	1.153	1.094	1.096	1.061	1.083	1.328
$R_1{}^{a,d}$	0.038	0.0301	0.034	0.0397	0.0295	0.0483
$wR_2{}^{b,e}$	0.1193	0.077	0.0917	0.1131	0.0798	0.1482
Flack parameter				0.03(6)	0.06(3)	
largest difference peak and hole (e Å^{-3})	0.883 and −0.431	0.746 and −0.536	1.165 and −0.822	0.760 and −0.513	0.566 and −0.563	1.264 and −1.783

[a] $F_o^2 \geq 2\sigma(F_o^2)$ [b] $F_o^2 \geq 3\sigma(F_o^2)$ [c] $S = [\Sigma w(F_o^2 - F_c^2)^2/(n-p)]^{1/2}$ [d] $R_1 = \Sigma||F_o| - |F_c||/\Sigma|F_o|$ [e] $wR_2 = [\Sigma w(F_o^2 - F_c^2)^2/\Sigma w(F_o^4)]^{1/2}$ [f] Distances involving the minor-occupancy of the counterion were constrained to be equal (within 0.001 Å) during refinement and/or constrained to the requisite geometry. [g] The geometry of the minor component (30%) of the disordered ligand was restrained to be the same as that of the major component (70%) by use of the SHELXL SAME instruction during refinement.

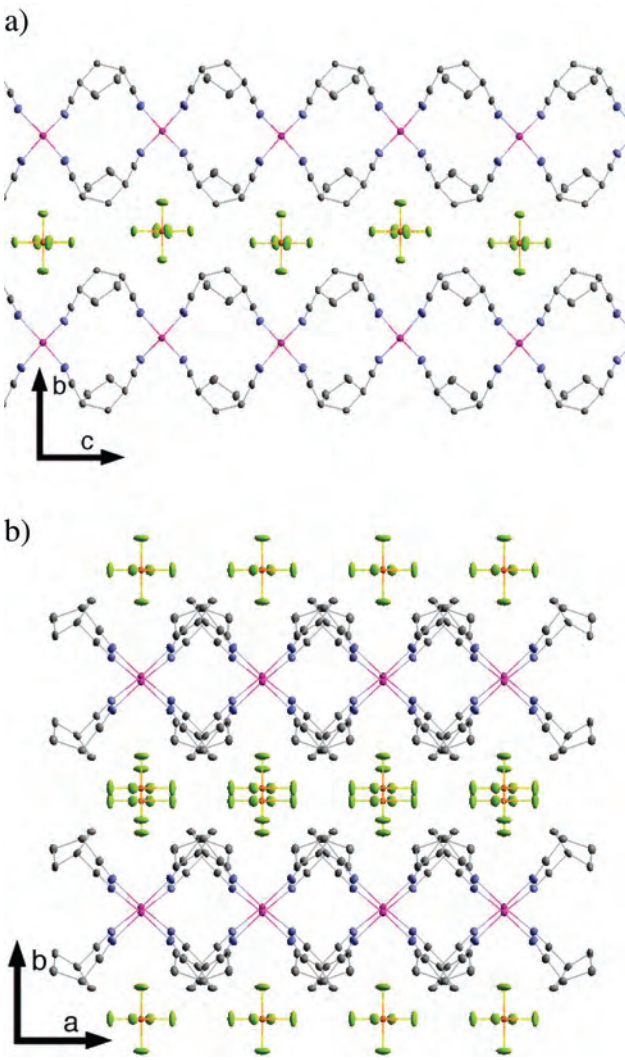

Figure 2. (a) Extended structure of **6b**, viewed along the *a*-axis. The chain extends along the *c*-axis and lies in the *bc*-plane. (b) Complex **6b**, viewed along the *c*-axis to reveal the *ab*-plane. The chains crystallize side by side to form sheets separated by rows of PF_6 anions.

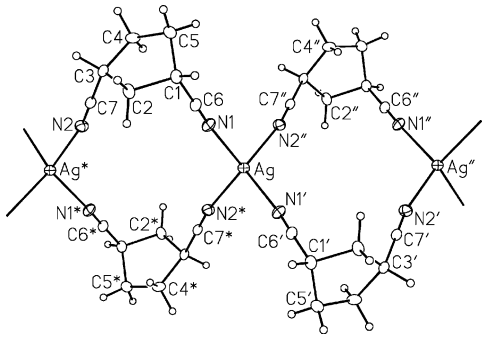

Figure 3. An ORTEP drawing of $[Ag(cpdcn)_2]^+$ **6b** with the atom labeling scheme. Non-hydrogen atoms are represented by Gaussian ellipsoids at the 20% probability level. Hydrogen atoms are shown with arbitrarily small thermal parameters. Symmetry modes: primed atoms: 0, *y*, $^1/_4$; double-primed atoms: *x*, 1 − *y*, $-^1/_2 + z$; starred atoms: 0, $^1/_2$, $^1/_2$.

= ClO_4^- $\rho = 1.750$ g/cm^3, Y = PF_6^- $\rho = 1.862$ g/cm^3, and Y = SbF_6^- $\rho = 2.094$ g/cm^3), the chains pack very efficiently into sheets. One chain is related to the next by translation of approximately 5.8−6.0 Å or one unit cell.

In each case, the asymmetric unit consists of one silver center, one ligand, and one counterion; the labeling scheme used is shown in Figure 3. The silver center has distorted tetrahedral geometry, and all metal atoms are bridged by two cpdcn ligands. Bond lengths and angles for these complexes are given in Table 3. No close Ag···Ag contacts are observed in the polymeric chain. Ag···Ag separations are approximately 6.466 Å (ClO_4^-), 6.542 Å (PF_6^-), and 6.693 Å (SbF_6^-) apart, where the slightly elongated Ag···Ag distance in SbF_6^- is thought to be due to the different space

Table 3. Selected Interatomic Distances (Å) and Angles (°) for Complexes **6a**−**c**

	6a	6b	6c
Ag−N1	2.2551(13)	2.282(3)	2.276(4)
Ag−N1′	2.2551(13)	2.282(3)	2.276(4)
Ag−N2″	2.2798(13)	2.260(2)	2.291(4)
Ag−N2*	2.2799(14)	2.260(2)	2.291(4)
N1−C6	1.136(2)	1.136(4)	1.131(6)
N2−C7	1.1359(19)	1.133(4)	1.135(6)
N1−Ag−N1′	104.20(7)	105.59(15)	100.5(2)
N1−Ag−N2″	117.89(5)	100.57(10)	116.89(15)
N1−Ag−N2*	109.36(5)	117.05(10)	113.54(16)
N1′−Ag−N2″	109.36(5)	117.06(10)	113.54(16)
N1′−Ag−N2*	117.89(5)	100.57(10)	116.89(15)
N2″−Ag−N2*	98.83(7)	116.29(14)	96.5(2)
Ag−N1−C6	166.87(15)	166.1(3)	170.8(4)
Ag″−N2−C7	164.59(14)	166.2(3)	165.4(4)

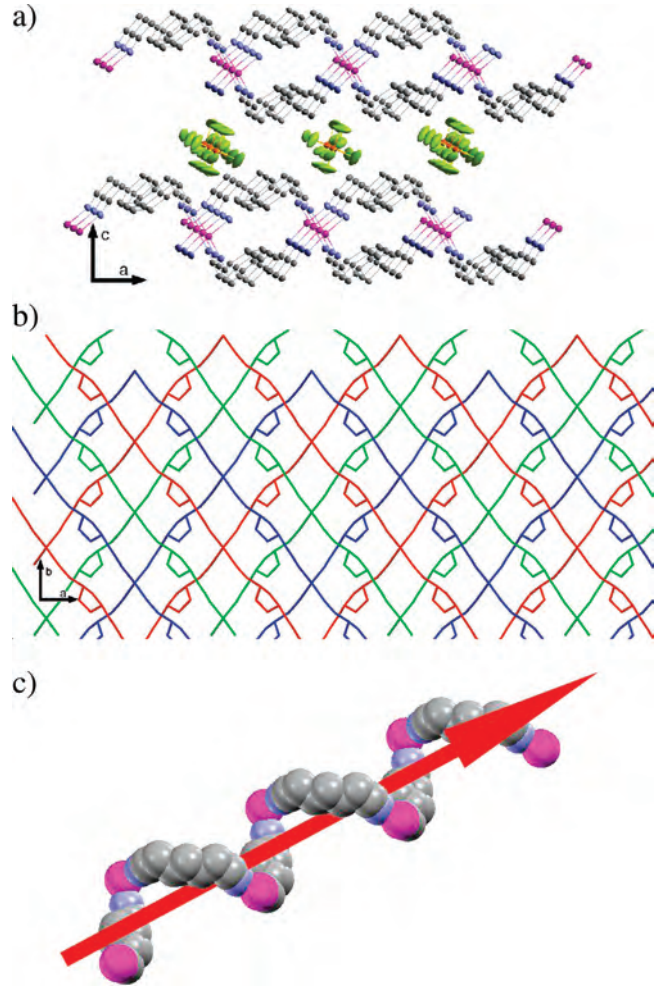

Figure 4. (a) Extended structure of **7b**. The chains extend along the *a*-axis and lie in the *bc*-plane. The 2D-layers are separated by rows of PF_6 anions. (b) The 3-fold parallel interpenetration for **7b**. (c) A perspective view of **7b** illustrating the left-handed helical nature of the polymer strands.

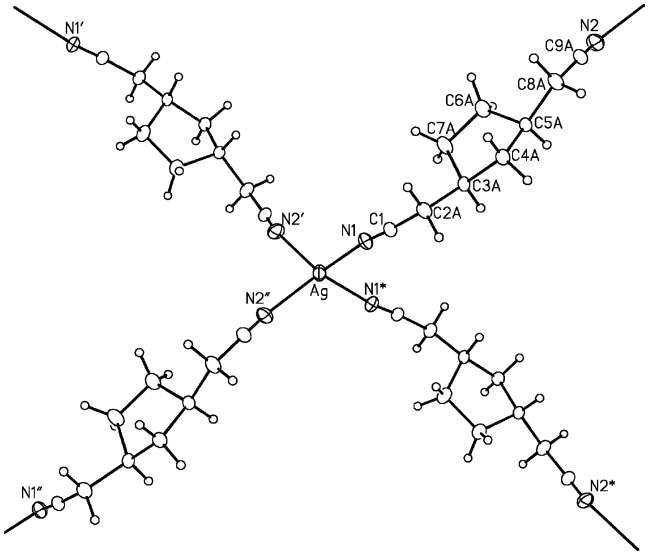

Figure 5. An ORTEP drawing of $[Ag(bcmcp)_2]^+$ **7b** with the atom labeling scheme. Only the major orientation (70%) of the disordered ligand is shown for clarity. Non-hydrogen atoms are represented by Gaussian ellipsoids at the 20% probability level. Hydrogen atoms are shown with arbitrarily small thermal parameters. Symmetry modes: Primed atoms: $^1/_2 - x$, $^3/_2 + y$, $\bar{z}$; double-primed atoms: $x - {}^1/_2$, $^3/_2 + y$, z; starred atoms: 0, y, 0; atoms marked with #: $x + {}^1/_2$, $y - {}^3/_2$, z.

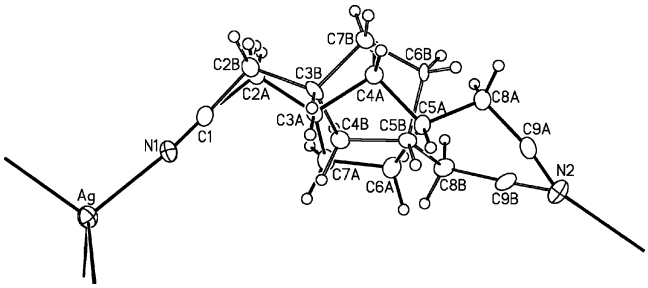

Figure 6. Diagram showing the two orientations of the disordered bcmcp ligand in complex **7b**, with the major (70%) form indicated by the solid bonds and the minor (30%) by the open bonds.

group.[25] The average Ag−N, C≡N and N−C bond distances are normal, comparing favorably to previously published data.[9–15] The five-membered ring in the ligand backbone adopts an envelope conformation with C1, C5−C3 atoms lying essentially coplanar.

X-ray Single Crystals of Complexes 7a and 7b. The increased flexibility afforded by the extra methylene groups in the ligand backbone of ditopic ligand bcmcp **2** yielded two different modes of self-assembly in the resultant Ag(I) coordination polymers **7a**−**c**. Complexes **7a** and **7b** are structurally quite similar in nature whereas complex **7c** is remarkably different. While crystals of $\{[Ag(bcmcp)_2]ClO_4\}_n$ **7a** were isolated from the reaction mixture, crystals of $\{[Ag(bcmcp)_2]ClO_4\}_n$ **7b** were grown by slow evaporation from a concentrated solution of acetone layered with ethanol. Complex **7a** crystallizes in an orthorhombic unit cell and is solved in the chiral space group $C222_1$, whereas complex **7b** crystallizes in a monoclinic unit cell and is solved in the chiral space group $C2$. In both complex **7a** and **7b**, each bcmcp ligand bridges two silver centers propagating a two-

(25) Fortin, D.; Drouin, M.; Turcotte, M.; Harvey, P. D. *J. Am. Chem. Soc.* **1997**, *119*, 531.

Table 4. Selected Interatomic Distances (Å) and Angles (°) for Complexes **7a**−**c**

	7a	**7b**
Ag−N1	2.296(7)	2.294(3)
Ag−N1*	2.296(7)	2.294(3)
Ag−N2′	2.25(2)	2.273(3)
Ag−N2″	2.25(2)	2.273(3)
N1−C1	1.119(11)	1.130(5)
N2−C9A	1.20(4)	1.171(6)
N1−Ag−N1*	107.4(4)	100.96(16)
N1−Ag−N2′	100.1(8)	122.31(12)
N1−Ag−N2″	125.6(8)	106.51(12)
N1*−Ag−N2′	125.6(8)	106.51(12)
N1*−Ag−N2″	100.0(8)	122.31(12)
N2′−Ag−N2″	100.6(15)	99.9(2)
Ag−N1−C1	171.0(8)	172.3(3)
Ag#−N2−C9A	170(2)	158.7(4)
C5A−C1A−C6A−C7A	68.7(8)	

	7c
Ag−N1	2.294(3)
Ag−N1*	2.294(3)
Ag−N2′	2.273(3)
Ag−N2″	2.273(3)
N1A−C1A	1.140(12)
N1A−Ag−N1A′	107.5(2)
N1A−Ag−N1A″	107.5(2)
N1A−Ag−N1A*	113.5(4)
N1A′−Ag−N1A″	113.5(4)
N1A′−Ag−N1A*	107.5(2)
N1A″−Ag−N1A*	107.5(2)
Ag−N1A−C1A	159.7(8)
C1A−C2A−C4A−C5A	−176.5(9)

dimensional coordination polymer as shown in Figure 4a. The topology of the network as represented by the Ag-to-Ag connectivity is a chiral (4,4) square mesh. The polymer consists of layers of rhombi with Ag−Ag edges of 12.168 Å (ClO_4^-) and 12.300 Å (PF_6^-) and diagonals of 18.681 Å and 15.598 Å (ClO_4^-) and 18.779 Å and 15.889 Å (PF_6^-) (see Figure 4b). The chirality can be easily appreciated from

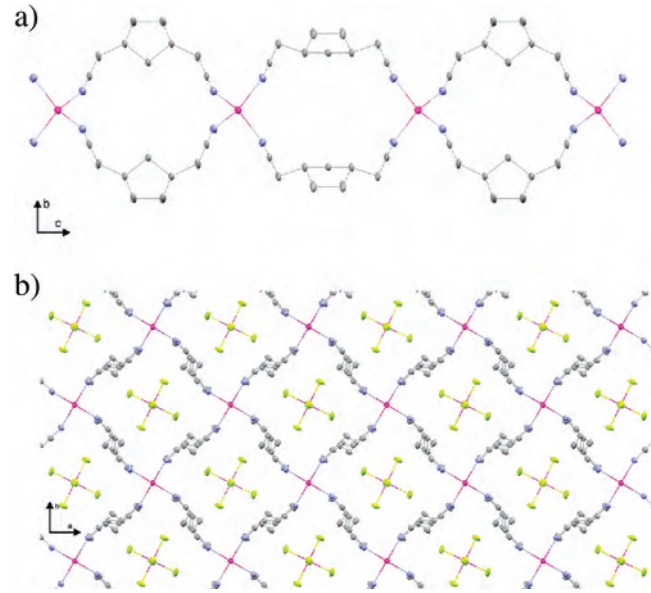

Figure 7. (a) Extended structure of **7c**. The chain extends along the *c*-axis and lies in the *bc*-plane. Hydrogens have been omitted for clarity. (b) The complex **7c** viewed down the *c*-axis. The anions are clathrated between strands of the 1D polymers.

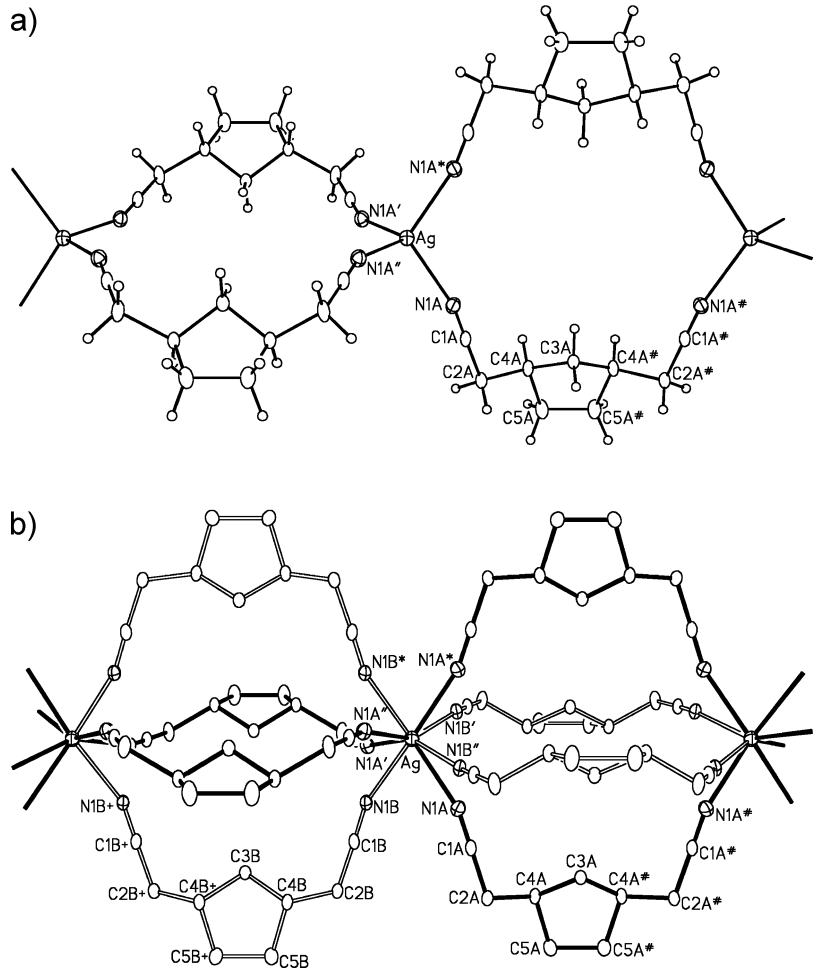

Figure 8. (a) An ORTEP drawing of $[Ag(bcmcp)_2]^+$ **7c** with the atom labeling scheme. Only the major orientation (70%) of the disordered ligand is shown for clarity. Non-hydrogen atoms are represented by Gaussian ellipsoids at the 20% probability level. Hydrogen atoms are shown with arbitrarily small thermal parameters. Symmetry modes: Primed atoms: $\bar{y} + {}^1/_2, x - {}^1/_2, \bar{z} + {}^1/_2$; double-primed atoms: $y + {}^1/_2, \bar{x} + {}^1/_2, \bar{z} + {}^1/2$; starred atoms: $\bar{x} + 1, \bar{y}, z$; atoms marked with #: $x, y, \bar{z} + 1$. (b) View showing the relationship between the major and minor orientations. The major form is drawn with solid bonds; the minor form with hollow bonds. Hydrogen atoms have been removed for clarity.

Figure 4c, where a single strand of the polymeric chain is viewed along the *a*-axis. Each channel created by the rhombus structure is helical in nature (left-handed), the helicity being generated by the silver atoms which act as hinges in the polymer structure. Three equivalent and independent strands of polymer are observed that interpenetrate in a parallel manner (see Figure 4b). For chiral (4,4)-layers, a degree of interpenetration higher than two based on coordinative bonds is exceptionally rare, with only one other case reported in the literature.[26] Unique to this case, however, is that each polymeric sheet is C_2-symmetric. Furthermore, the helical channels of the three interpenetrating networks are parallel to one another and have the same hand in each direction, preserving the overall chirality of the material. Interestingly, only three cases of 3-fold parallel interpenetration have been observed for achiral polymers,[27] two of which are reported by Ciani.[11]

The asymmetric unit of complexes **7a** and **7b** consists of one silver center, two ligands, and one counterion; the labeling scheme used is shown in Figure 5. As is the case in many dinitrile silver complexes,[11] the ligands are disordered. It was possible to resolve the minor occupancy which can be seen in Figure 6. The silver centers have distorted tetrahedral geometry (NAgN $\angle$ = 100.0(8)−125.6(8)° (ClO_4^-), 99.9(2)−122.31(12)° (PF_6^-)) and the average Ag—N, C≡N, and N—C bond distances are normal.[9–15] Bond lengths and angles for these complexes are given in Table 4. No close Ag···Ag contacts are observed in the polymeric chain. The closest Ag···Ag separations between polymer chains in the helical structure are 6.227 Å (ClO_4^-) and 6.260 Å (PF_6^-) apart. The five-membered ring in the ligand backbone adopts an envelope conformation with C1, C5−C3 atoms lying essentially coplanar.

X-ray Single Crystal of Complex 7c. Despite identical reaction conditions and recrystallization conditions to $\{[Ag(bcmcp)_2]PF_6\}_n$ **7b** (two factors known to affect supramolecular interactions in the self-assembly process), the resulting crystal structure for $\{[Ag(bcmcp)_2]SbF_6\}_n$ **7a** is solved in the achiral space group *I*4/*m*. The $[Ag(bcmcp)_2]^+$ units in the crystal exist as a series of 1D polymers in which silver atoms form the basis for the linear straight chain (AgAgAg $\angle$ = 180°, Figure 7a) propagating along the *c* axis.

(26) Lin, W. B.; Evans, O. R.; Xiong, R. G.; Wang, Z. Y. *J. Am. Chem. Soc.* **1998**, *120*, 13272.
(27) Ge, C. H.; Zhang, X. D.; Zhang, P.; Guan, W.; Guo, F.; Liu, Q. T. *Polyhedron* **2003**, *22* (27), 3493–3497.

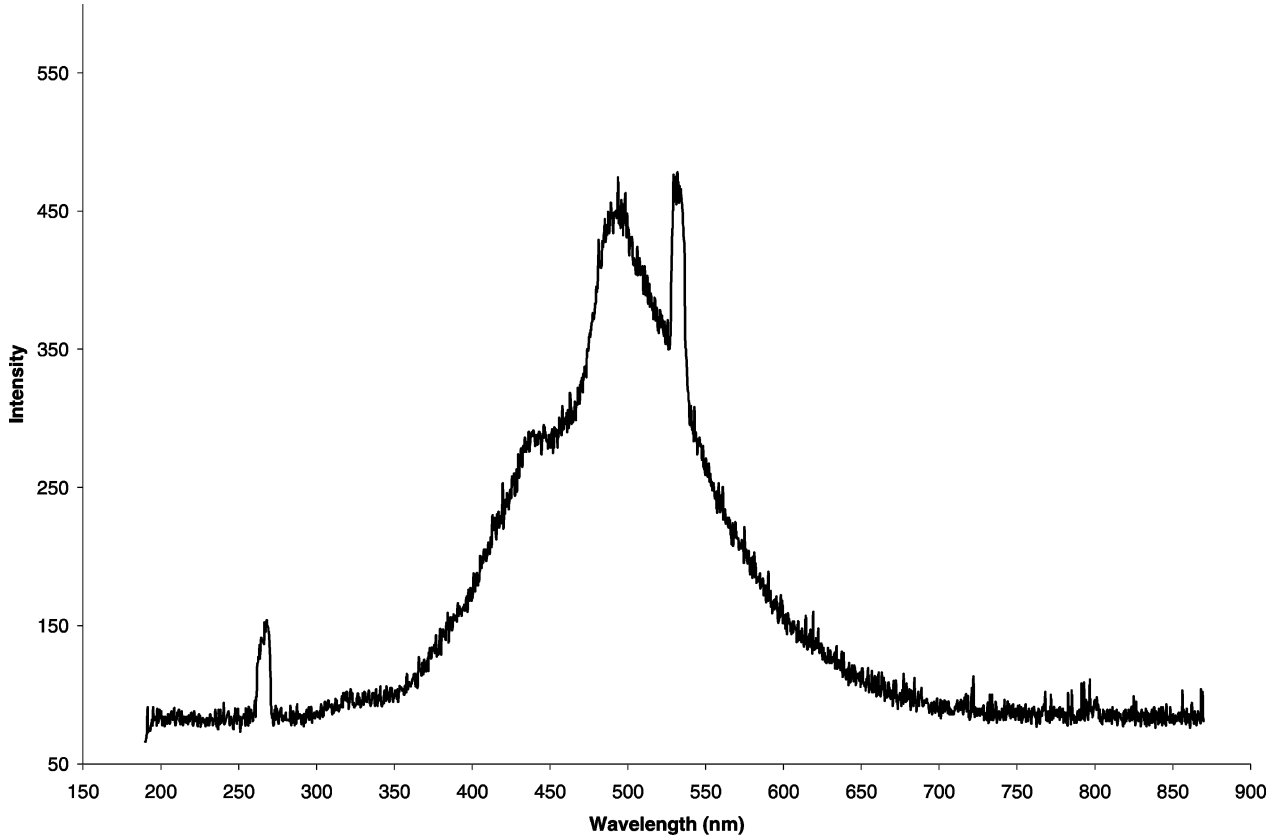

Figure 9. Solid state emission spectra for complex **7a**.

The chains crystallize very efficiently in the unit cell (ρ_{calcd} = 1.848 g/cm^3); each chain is related to the next by a rotation of 90° along the *c*-axis and can be located along either the *b* or *a* axis. As the silver atoms of each chain all lie in the same *ab* plane, square cavities are formed into which the counterions are clatherated (see Figure 7b).

The asymmetric unit of complex **7c** consists of one silver center, one-half of one ligand, and one counterion; the labeling scheme used is shown in Figure 8a. The bcmcp ligand is disordered and the minor occupancy (30%) can be seen in Figure 8b. There are no contacts between the silver atoms within the polymeric chain; Ag···Ag separations are approximately 9.143 Å apart. In fact, the Ag···Ag distance between chains is closer, measuring 7.931 Å. Each Ag atom is coordinated in a mildly distorted tetrahedral environment (NAgN ∠ = 107.5(2)−113.5(4)°). The average Ag−N bond length at 2.268(8) Å and the C≡N bond length at 1.140(12) Å are normal; the Ag−N≡C bond angle, however, is rather acute at 159.7(8)°. The five-membered ring in the ligand backbone adopts an envelope conformation with C4A/A# andC5A/A# atoms lying essentially coplanar. Bond lengths and angles for complex **7c** are given in Table 4.

It is apparent that the major difference between the extended structures observed in complexes **7a** and **7b** relative to **7c** is due to the rotational freedom of the methylene groups linking the nitrile to the cyclopentane ring in the ligand backbone of bcmcp **2**. This change in conformation is likely triggered by the change in counterion.[5,28–30] The torsional angle (−176.5(9)°) between the nitrile carbon and C5A indicates an anti conformation between these two atoms in complex **7c**. In complexes **7a** and **7b**, these torsional angles are measured to be 68.7(8)° and 56.9(6)°, respectively.

Photoluminescence Data. A preliminary investigation into the solid state photoluminescence of complexes **6a**−**c** and **7a**−**c** was undertaken. All complexes were observed to be weakly luminescent at room temperature. Figure 9 illustrates a luminescence emission spectrum of complex **7a**, typical of all the emission spectra observed for complexes **6a**−**c** and **7b**,**c**. The solid state spectrum for complex **7a** shows a broad emission band centered on 497 nm with a shoulder appearing at 441 nm. Surprisingly, supramolecular influences do not seem to affect the emission spectra.[14,31,32] As a result, it is speculated that the emission spectra observed arises from metal to ligand charge transfer.[14]

Conclusions

A significant focus of this work has been the comparison of a rigid aliphatic dinitrile ligand to a semirigid ligand in the coordination chemistry of silver(I). The use of aliphatic structurally rigid *meso*-dinitrile ligand cpdcn **1** coordinated

(28) Kim, H. J.; Zin, W. C.; Lee, M. *J. Am. Chem. Soc.* **2004**, *126*, 7009.
(29) Blake, A. J.; Baum, G.; Champness, N. R.; Chung, S. S. M.; Cooke, P. A.; Fenske, D.; Khlobystov, A. N.; Lemenovskii, D. A.; Li, W. S.; Schroder, M. *J. Chem. Soc., Dalton Trans.* **2000**, (23), 4285.
(30) For counterion effects on chiral Ag(I) coordination polymers see: (a) Blake, A. J.; Champness, N. R.; Cooke, P. A.; Nicolson, J. E. B.; Wilson, C. *J. Chem. Soc., Dalton Trans.* **2000**, (21), 3811.
(31) Perreault, D.; Drouin, M.; Michel, A.; Harvey, P. D. *Inorg. Chem.* **1992**, *31*, 3688.
(32) Harvey, P. D. *Macromol. Symp.* **2004**, *209*, 81.

to the silver salts in this study resulted in the formation of thermally stable, chiral 1D-coordination polymers regardless of the counterion or recrystallization solvent used. Most often conjugated rod-like or planar ligands have been used to produce predictable Ag(I) polymeric architectures;[5] this work illustrates that judicious choice of rigid aliphatic ligands result in structures that appear unaffected by many of the factors that can influence self-assembly, allowing for greater architectural control of extended structures. In contrast, the semirigid ligand bcmcp **2** offers a higher degree of conformational freedom. This is evident in the resulting complexes that were observed to self-assemble when bcmcp was coordinated to Ag(I). The structures of complexes **7a** and **7b** are best described as a 2D chiral (4,4) square mesh with 3-fold parallel interpenetration, while complex **7c** was characterized to be an achiral 1D coordination polymer.

Acknowledgment. E.D.G. and J.A.K. are appreciative of Undergraduate Student Research Awards from the Natural Science and Engineering Research Council (NSERC). Financial support for this work from NSERC and The King's University College is gratefully acknowledged.

Supporting Information Available: This material is available free of charge via the Internet at http://pubs.acs.org.

IC800069F